

# Real-Time Condition Monitoring of Transmission Line Insulators Using the YOLO Object Detection Model With a UAV

Satyajit Panigrahy<sup>ID</sup>, *Graduate Student Member, IEEE*, and Subrata Karmakar<sup>ID</sup>, *Senior Member, IEEE*

**Abstract**—Continuous monitoring and inspection of high-voltage insulators are necessary to prevent failures and emergencies. Manual inspections can be costly and time-consuming, particularly when covering large geographical areas exposed to harsh weather conditions. This study proposed a single-stage object detector approach to address the limitations of traditional inspection methods by utilizing a hexacopter for efficient inspections of outdoor insulators. The object detector model was trained using a dataset of 6020 insulator images for detecting defects in complex backgrounds. Image augmentation techniques were adopted to avoid overfitting. Finally, the hexacopter was equipped with an onboard camera and a Raspberry Pi 4 single-board computer to automate the outdoor insulator inspection system by detecting real-time defects. Experimental results demonstrated the effectiveness of the YOLov8n object detector model in successfully identifying various insulator conditions, including normal, broken, polluted, and flashover surfaces, with a mAP@50 of 99.4%.

**Index Terms**—Outdoor insulators, raspberry Pi 4 (IoT), remote condition monitoring, single-stage object detection, UAV (hexacopter), you only look once (YOLO).

## I. INTRODUCTION

INSULATORS have an important function in the operation of transmission lines, as they offer both isolation and mechanical support to the power line conductors. Due to prolonged exposure to the outdoor environment, insulators are susceptible to electrical, mechanical, and thermal stresses that arise from different environmental conditions [1]. The aforementioned stresses can result in the deterioration of surface resistance, flashover voltage, and puncture strength, resulting in increased leakage current and a decline in insulation strength. Such failure of insulators can have far-reaching consequences, impacting the functioning of the entire power system and leading to extensive power outages that entail significant economic losses. Hence, timely identification and replacement of faulty insulators become crucial [2]. Conventional insulator monitoring approaches, such as manual patrol and helicopter investigations, are slow, costly, and potentially hazardous. They rely on subjective visual observation skills and may have limited detection rates. Climbing robots can also

Manuscript received 29 December 2023; revised 13 February 2024; accepted 4 March 2024. Date of publication 25 March 2024; date of current version 4 April 2024. The Associate Editor coordinating the review process was Dr. Anant Kumar Verma. (*Corresponding author: Subrata Karmakar*.)

The authors are with the Department of Electrical Engineering, National Institute of Technology, Rourkela, Odisha 769008, India (e-mail: karmakar.subrata@gmail.com).

Digital Object Identifier 10.1109/TIM.2024.3381693

cause damage to power lines due to its weight. To overcome these limitations, alternative approaches are needed to enhance efficiency and safety in insulator protection in power transmission systems [3].

Machine learning techniques were developed for insulator defect classification by extracting the features from the images to overcome the difficulties of the traditional methods. Pernebayeva et al. [4] utilized image normalization filters and machine learning classifiers to assess the state of outdoor glass insulators in harsh winter conditions and polluted environments. It is observed that the machine learning algorithms relied on manually selected features, leading to challenges in consistently obtaining good detection results. This issue was addressed by convolutional neural networks (CNNs), which automatically learn and extract features from images, including texture, shape, and patterns. Tao et al. [5] developed a two-level CNN architecture for insulator localization and defect detection, necessitating intensive hyperparameter tuning and optimization at each stage. In response to the challenges associated with cascaded CNNs, research has explored image preprocessing techniques, such as transfer learning, image augmentation, and low-light enhancement. Cao et al. [6] introduced an efficient method for detecting glass insulator defects, with a focus on self-detonation defects, while Yuan et al. [7] presented a novel algorithm to significantly enhance contrast in low-light images, specifically targeting object detection in overhead power transmission systems. This algorithm led to a notable increase in detection accuracy, from 58.0% to 82.0%. Overall, image preprocessing techniques significantly contribute to mitigating the limitations of CNN models by enhancing image quality, reducing noise, and improving generalization capabilities.

In recent years, object detection has witnessed significant advancements in model architectures. Earlier approaches, such as R-CNN and SSD models, relied on complex multistage pipelines, resulting in computational inefficiencies and slower inference times. Zhao et al. [8] presented an enhanced Faster R-CNN algorithm for insulator recognition and fault detection, utilizing a combination of Faster R-CNN and improved FPN. The experimental results demonstrated a mean average precision (mAP) of 90.8% for glass insulators and 91.7% for composite insulators on the testing dataset. Miao et al. [9] utilized a deep learning-based approach employing a single-shot detector (SSD) to automatically detect insulators in aerial images for power transmission

line inspection. Their SSD-based model uses automatic multilevel feature extraction from aerial images, eliminating the need for manual feature extraction. In addition, a two-stage fine-tuning strategy inspired by transfer learning significantly enhances accuracy, efficiency, and robustness. However, the emergence of you only look once (YOLO) models has revolutionized object detection by introducing a single-stage architecture, offering improved speed and efficiency. Sadykova et al. [10] introduced a YOLOv2 neural network model for insulator detection and classification based on surface conditions but struggled with detecting small objects due to its fixed grid size. Zhang et al. [11] achieved an mAP at a 50% threshold of 97.76% using the YOLOv3 model on a public dataset to detect the missing insulator cap, benefitting from YOLOv3's variable grid size and aspect ratio features. The YOLOv3 model suffered from a limitation where the weights could not be learned independently. In response, the YOLOv4 model was introduced, addressing this drawback by implementing multiple detection heads and anchor box clustering to enhance overall detection performance. Researchers further improved YOLO's efficiency by replacing the backbone network with advanced models, such as MobileNetv3, for edge device implementation, achieving high detection accuracy and speed [12]. Hybrid YOLO models, such as YOLO-ResNet-18 [13], displayed enhanced object detection capabilities, striving to achieve an optimal balance between speed and accuracy in various applications, including power system inspection and insulator defect detection. Furthermore, Zheng et al. [14] enhanced insulator defect detection using YOLOv7 by replacing the default anchor box size with K-means++ clustering. This modification exemplifies the continuous evolution of object detection technology, emphasizing the pursuit of superior speed and accuracy to address the diversity of objects in real-world scenarios.

In recent years, the integration of UAVs and embedded systems has revolutionized real-time inspection and monitoring of power transmission components. This synergy has enabled the automated inspection of high-voltage insulators in challenging and remote locations, significantly reducing the necessity for manual checks while enhancing the overall reliability of power distribution networks. Waleed et al. [15] devised a quadcopter-based system to classify ceramic insulators as healthy, broken, or dirty. However, limitations in detecting healthy insulators in onshore processing mode were observed, with mAPs of 0.67 onshore and 0.26 onboard. To address this, Rahman et al. [16] proposed a solution using image augmentation, super-resolution, low-light enhancement, obstacle avoidance, UAV path planning, and YOLOv4 object detection. This approach achieved an *F1* score of 0.81 for detecting damaged insulators and a more efficient flight strategy. Furthermore, Song et al. [17] introduced a collaborative intelligent method combining cloud and edge computing for detecting insulator string defects, demonstrating good accuracy, albeit addressing only two defect types described in CPLID. To increase the functionality and effectiveness of insulator detection algorithms, researchers and developers are continuously looking into new methodologies and architectural designs. These advanced models and their variants will be

focused on future works to identify small-scale occluded insulators with defects.

The work's novelty encompasses several key contributions. First, it involves the curation of a comprehensive dataset featuring diverse defects, effectively addressing limitations in the existing public datasets. Second, image augmentation techniques enhance the dataset's robustness by simulating real-time conditions. Adopting an advanced single-stage object detection model also represents a significant methodological advancement over traditional models. Finally, the real-time monitoring tests with a hexacopter and Raspberry Pi IoT devices demonstrate an innovative hardware application for practical field implementation.

The salient aspects of this work are summarized as follows.

- 1) A comprehensive dataset of 6020 images of suspension-type porcelain insulators was acquired under varied positions, angles, and zooms to train the detector model better.
- 2) To address the overfitting of image data, 32 different types of image augmentation techniques were used during the image preprocessing stage.
- 3) The most advanced YOLOv8 model was employed in this work to monitor the insulator states, including clean, broken, polluted, and flashing surfaces.
- 4) In order to thoroughly evaluate the performance of the object detector, comprehensive tests were conducted using YOLO model variants. To specifically assess the robustness of the YOLOv8 model, an evaluation was carried out on insulator images from the insulator defect image dataset (IDID) and Chinese power line insulator dataset (CPLID) public datasets, which were untrained by the model.
- 5) Finally, the Raspberry Pi was programmed with the trained model algorithm and mounted on the hexacopter for real-time condition monitoring of the insulators.

The study proceeds as follows. Section II introduces the theoretical foundation of single-stage object detectors. Section III presents the proposed UAV system for real-time condition monitoring of the insulator defects. Section IV provides a detailed analysis of the experimental results obtained from evaluating the approach. Finally, Section V outlines the study's conclusion and offers recommendations for future research.

## II. OVERVIEW OF SINGLE-STAGE OBJECT DETECTION MODELS

Single-stage object detection models, such as YOLO, SSD, FCOS, RetinaNet, and EfficientDet, detect objects directly without the need for a separate region proposal network and classifier. This approach enables faster inference times compared with two-stage object detection models. YOLO, in particular, has gained significant attention for its real-time object detection capabilities [18]. Over the years, multiple versions of YOLO, including YOLOv1, YOLOv2, YOLOv3, YOLOv4, YOLOv5, YOLOv6, YOLOv7, and YOLOv8, have been introduced in Table I.

The latest version of the YOLO object detection model is YOLOv8. It is composed of a backbone, neck, and head, as depicted in Fig. 1.

TABLE I  
DETAILS OF THE YOLO MODEL

Model Name	Year	Anchor	Framework	Backbone
YOLOv1	2015	No	Darknet	Darknet24
YOLOv2	2016	Yes	Darknet	Darknet24
YOLOv3	2018	Yes	Pytorch	Darknet53
YOLOv4	2020	Yes	Darknet	CSPDarknet53
YOLOv5	2020	Yes	Pytorch	YOLOv5CSPDarknet
YOLOv6	2022	No	Pytorch	EfficientRep
YOLOv7	2023	No	Pytorch	YOLOv7Backbone
YOLOv8	2023	No	Pytorch	YOLOv8CSPDarknet

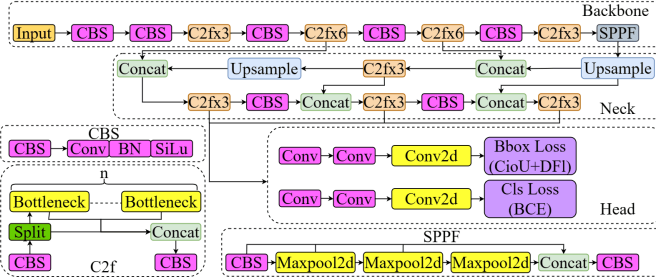


Fig. 1. Architecture of YOLOv8.

### 1) Backbone:

- a) In YOLOv8, the architecture utilizes the CSPDarknet framework. Instead of the CSP module from the original backbone network, the C2f module is employed.
- b) The C2f module in YOLOv8 incorporates a gradient shunt connection. This connection enhances the information flow within the feature extraction network, while keeping the module lightweight.
- c) The CBS module in YOLOv8 applies convolution, batch normalization, and SiLU activation to process the input information and produce the output result.
- d) The backbone network of YOLOv8 incorporates the SPPF module, which performs adaptive size output by pooling the input feature maps into a fixed-size map.

### 2) Neck:

- a) The neck architecture in YOLOv8 utilizes PAN-FPN, which incorporates a hybrid approach of top-down and bottom-up network structures. This fusion of shallow positional and deep semantic information enhances feature diversity and completeness, resulting in improved performance.

### 3) Head:

- a) The detection part utilizes a decoupled head structure with two separate branches. One branch focuses on object classification, while the other handles predicted bounding box regression. This separation allows for a more accurate and efficient detection process.
- b) YOLOv8 utilizes binary cross-entropy loss (BCE Loss) for the classification task.
- c) In the predicted box bounding regression task of YOLOv8, distribution focal loss (DFL) and CIoU (complete IoU) are utilized.

The YOLOv8 model has five versions: YOLOv8n (nano), YOLOv8s (small), YOLOv8m (medium), YOLOv8l (large), and YOLOv8x (extra large). Depth and width multiple parameters are used to achieve the size variations.

### III. UAV-ASSISTED INSULATOR CONDITION MONITORING SYSTEM

The explanation of dataset formation, image preprocessing using image augmentation methods, image annotation, hexacopter design, and system configuration used for the test performance is explained in this section. The procedural steps for monitoring the state of the insulator are illustrated in Fig. 2 and explained as follows.

- 1) The dataset of suspension-type porcelain insulators includes images captured using a camera with varying zoom and angle conditions. It covers clean, polluted, broken, and surface defect conditions with single- and multidisk combinations.
- 2) In the second stage, image augmentation techniques are used to generate multiple variations of the original images. This increases the dataset size, prevents overfitting, and improves the model's ability to generalize to unseen data.
- 3) All the preprocessed images are labeled manually according to their surface condition before being sent to the single-stage object detector.
- 4) In the fourth stage, single-stage deep-learning object detector models are trained with the labeled images collected after the image annotation stage.
- 5) Finally, hexacopter along with Raspberry Pi 4 is deployed for the real-time inspection of the outdoor insulator.

#### A. Insulator Image Dataset Preparation

The study utilized porcelain insulators sourced from the Aditya Birla Group. These insulators have a 90-KN electromechanical strength, with a creepage distance of 430 mm. The disk diameter is 255 mm, and the unit spacing is 145 mm. The experiment involved a total of 6020 insulator detection images, with 4900 acquired by the camera and 1120 created through image data augmentation. The insulators captured by the camera were formed by varying the positions of the disks among five places in the insulator string. In addition, 19 camera filters and two zoom levels (1× and 2×) were utilized. The dataset was divided into a training set, comprising 4816 images, and a test set with 1204 images, maintaining an 80:20 ratio. Fig. 3(a) shows the different surface conditions of the insulators, with surface defects and broken sheds obtained from long-term service insulators, and polluted insulators artificially generated in the laboratory. Fig. 3(b) depicts the combinations of insulators used to form the image dataset for detector model training.

#### B. Image Augmentation

Image augmentation expands the diversity and volume of training data. This is particularly important in scenarios where the available dataset is limited, as it enables the model to learn from a wider array of variations and conditions, improving

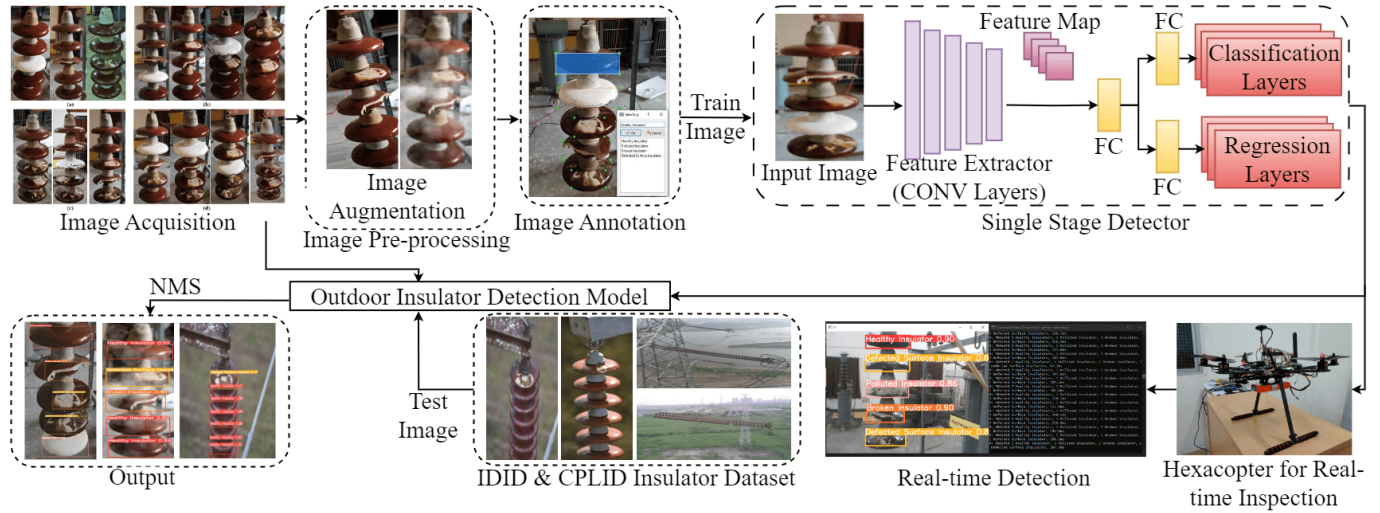


Fig. 2. Illustration of the Proposed Method.



Fig. 3. Insulator surface conditions. (a) Individual defects. (b) Combined defects.

TABLE II  
LIST OF IMAGE AUGMENTATION TECHNIQUES

Augmentation	Augmenter
Meta	Sometimes, With Channels, Channel Shuffle, Lambda
Arithmetic	Additive Gaussian Noise, Dropout, Impulse Noise, Salt & Pepper
Blend	Alpha, Checkerboard, Simple Noise, Some Colours
Blur	Gaussian Blur, Bilateral Blur, Motion Blur, Mean Shift Blur
Convolutional	Sharpen, Emboss, Edge Detect, Directional Edge Detect
Geometric	Affine, Scale, Translate, Rotate
Contrast	Gamma, Sigmoid, CLAHE, ACHE
Weather	Cloud, Fog, Snowflake, Rain

its ability to generalize and recognize objects accurately in real-world scenarios. In addition, image augmentation mitigates overfitting by introducing variability, enhancing the model's robustness and performance on unseen data. This study employed 32 augmenters from eight augmentation categories using the ImgAug tool [19], as outlined in Table II. The process of image augmentation using that tool is outlined in Algorithm 1. The resulting augmented insulator images are depicted in Fig. 4.

### C. Image Annotation

Image annotation is critical in object detection, as it provides the necessary ground-truth labels for training deep

### Algorithm 1 Image Augmentation Using ImgAug

- 1: **Load Images:**  
2: - Load original images.
- 3: **Define Augmentation Pipeline:**  
4: - Choose augmentation techniques and parameters.
- 5: **Apply Augmentation:**  
6: - Iterate through each image.  
7: - Apply selected augmentation techniques.
- 8: **Save Augmented Images:**  
9: - Save augmented images.
- 10: **Iterate or Finalize:**  
11: - Adjust augmentation parameters if necessary.  
12: - Finalize augmented dataset for training.

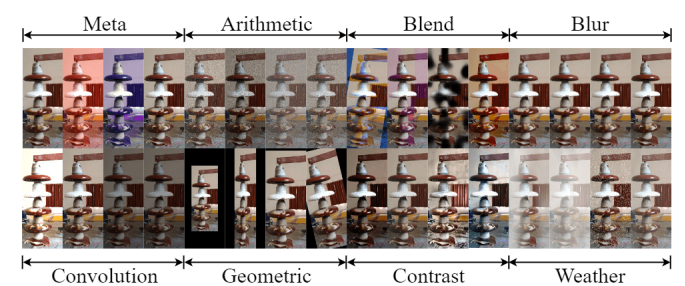


Fig. 4. Illustration of the image augmentation method.

learning models. By accurately marking objects and their boundaries within images, annotation facilitates the model's understanding of various objects and their spatial characteristics. This study utilized the LabelImg image annotation tool to annotate the insulator conditions. It saves the annotations in .txt files using the YOLO format. The procedure for image annotation using this tool is detailed in Algorithm 2, and the tool's graphical user interface is shown in Fig. 5.

### D. Hexacopter Setup

In this study, a custom-designed hexacopter was employed for monitoring outdoor insulator conditions, illustrated in Fig. 6. The hexacopter is built on an S550 frame and

**Algorithm 2** Image Annotation Using LabelImg

- 1: **Open LabelImg:**
- 2: - Launch the LabelImg application.
- 3: **Load Images:**
- 4: - Import the images to annotate.
- 5: **Annotate Objects:**
- 6: - For each image:
- 7: - Click on the “Create RectBox” button to draw bounding boxes around objects of interest.
- 8: - Label each bounding box with the corresponding object class.
- 9: - Adjust the size and position of the bounding boxes as needed.
- 10: **Save Annotations:**
- 11: - Once all images are annotated, save the annotations in YOLO format.
- 12: **Iterate or Finalize:**
- 13: - If necessary, revisit images for additional annotations or corrections.
- 14: - Finalize the annotated dataset for training the models.

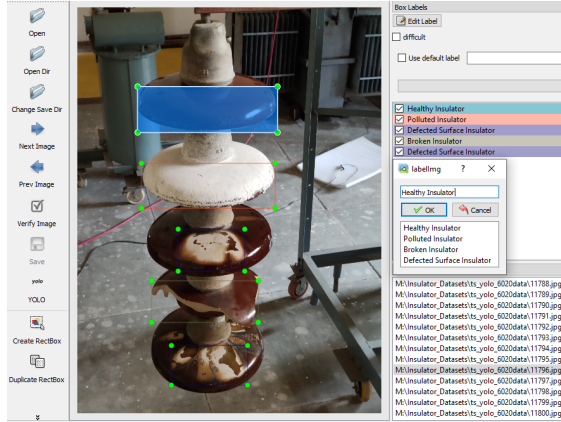


Fig. 5. LabelImg’s GUI for image annotation.

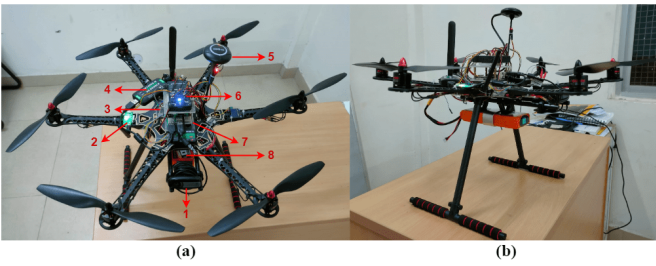


Fig. 6. Hexacopter view. (a) Top. (b) Side.

powered by a battery. The flight controller allows integration of sensors and enables autonomous flight using programs, such as Mission Planner or QGroundcontrol, flying to predetermined waypoints. Table III displays the components utilized in the design of the hexacopter.

The operational flow of the designed hexacopter system and its coordinated movement along transmission lines is depicted in Fig. 7. The drone’s default mode is to follow user-defined waypoints, each acting as a loiter point for 20 s. During these

TABLE III  
COMPONENTS OF HEXACOPTER

Tag No.	Part Name
1	Logitech C920 HD Pro Camera Module
2	433 MHz Radio Telemetry Receiver
3	PPM Encoder
4	4G Dongle for Raspberry Pi
5	GPS Module
6	Pixhawk Flight Controller
7	Raspberry Pi 4 Model B
8	8000 mAh, 3S, 11.1 V DC LiPo Battery

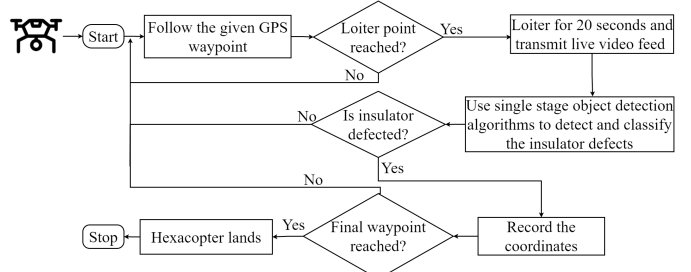


Fig. 7. Operational flow of the hexacopter system.

intervals, the onboard Raspberry Pi runs an object detection model to evaluate insulator conditions from the video feed. If any defects are detected, the drone’s GPS coordinates are recorded. If no defects are identified, the UAV will loiter for 20 s before progressing to the next waypoint until it reaches the final destination set by the mission planner. As a safety precaution, the mission planner is programmed to halt the inspection if the battery level drops to 20% and initiates the return to the starting point. The GPS coordinates are transmitted to the inspection team upon completion to facilitate prompt decision-making.

**E. Experimental Configuration**

The tests were conducted on a Windows 11 machine with an NVIDIA RTX 4090 GPU (24 GB memory) and 64 GB of RAM. In addition, the suggested method was evaluated on a Raspberry Pi 4 with 8 GB of RAM, a Quad-Core 64-bit Broadcom 2711, a Cortex A72 processor, and an Operating Power of 5V@3A over a Type-C USB port. The Raspberry Pi 4 was powered by the Raspbian operating system.

**IV. RESULTS AND DISCUSSION**

In this section, the focus was on presenting the experimental findings of the study. First, the performance of different YOLOv8 models was evaluated to identify a model with higher precision and lower complexity. Subsequently, a comparison was made between the YOLOv8 model and other YOLO models, highlighting the detection performance achieved for each class. Furthermore, the effectiveness of the proposed model was demonstrated through a comparison with Faster R-CNN, SSD model. In addition, a robustness study was conducted using two public datasets, namely, IDID and CPLID. Finally, the real-time implementation of the approach on a hexacopter was showcased.

TABLE IV  
PERFORMANCE EVALUATION OF YOLOv8 MODELS

Model Name	Precision	Recall	mAP @50	mAP @50-95	Params (M)	FLOPs
YOLOv8n	0.997	0.999	0.994	0.862	3.2	8.7
YOLOv8s	0.997	0.998	0.994	0.868	11.2	28.6
YOLOv8m	0.998	0.998	0.994	0.868	25.9	78.9
YOLOv8l	0.998	0.998	0.994	0.865	43.7	165.2
YOLOv8x	0.997	0.998	0.994	0.867	68.2	257.8

### A. Implementation Details

The model is implemented in PyTorch and trained for 50 epochs with a batch size of 32. The learning rate is set to 0.001, the NMS threshold is 0.45, and the IoU threshold is 0.5. The SGD optimizer is used with a momentum of 0.937 and a weight decay of 0.0005.

### B. Evaluation Metrics

This study employs several measures to assess the performance of the detection method. These measures include mAP@50, precision (P), recall (R), inference time, FLOP, number of parameters, and layers

$$P = \frac{\text{true positive}}{\text{all detection}} \quad (1)$$

$$R = \frac{\text{true positive}}{\text{all ground truths}} \quad (2)$$

$$\text{mAP} = \frac{1}{\text{classes}} \sum_{i=1}^N \text{average precision}_i. \quad (3)$$

In addition to detection metrics, classification evaluation metrics play a vital role in categorizing images into different classes. These metrics include accuracy, recall, F1 score, precision, kappa coefficient (k), Matthew's correlation coefficient (MCC), and Fowlkes–Mallows index (FM). They are calculated from the true positive, true negative, false positive, and false negative values obtained from the confusion matrix.

This study aims to identify the least complicated, lightest model with the best detection results. Table IV shows that, with 3 million parameters and 8.1 G Flops, YOLOv8n is less complex and lightweight than other models, making it simple to integrate into embedded systems for real-time detections. The condition assessments for individual insulator defect classes using various YOLO models are shown in Table V. The YOLOv8n detection model is better than previous YOLO models in terms of mAP@50-95. As can be seen from Table VI's overall performance comparison findings, our recommended model performs better than other models in terms of mAP@50 and inference time, which are 99.4% and 2.08 s, respectively. The detection result of the YOLO models for a test set image is shown in Fig. 8.

The insulator's healthy, polluted, broken, and flashing surface classes are represented in the 1204 test images in 3059, 620, 613, and 1728 instances each, for a total of 6020 instances ( $1204 \times 5$ ). These defect class categorizations are displayed in Fig. 9 as a confusion matrix, and the classification evaluation indices are provided in Table VII.

TABLE V  
PERFORMANCE EVALUATION OF YOLO MODELS FOR INDIVIDUAL CLASSES

Model Name	Class	Precision	Recall	mAP@50	mAP@50-95
YOLOv3	Healthy	0.999	0.979	0.979	0.82
	Polluted	0.996	0.997	0.994	0.788
	Broken	0.993	0.976	0.974	0.707
	Surface Defect	0.983	0.945	0.952	0.649
YOLOv5	Healthy	0.996	0.999	0.995	0.825
	Polluted	0.997	0.992	0.993	0.746
	Broken	0.976	0.983	0.979	0.682
	Surface Defect	0.947	0.944	0.98	0.626
YOLOv6	Healthy	0.998	0.998	0.995	0.874
	Polluted	0.997	0.987	0.993	0.854
	Broken	0.989	0.998	0.994	0.793
	Surface Defect	0.952	0.944	0.956	0.721
YOLOv7	Healthy	0.983	0.999	0.995	0.778
	Polluted	0.99	0.994	0.993	0.721
	Broken	0.975	0.969	0.974	0.622
	Surface Defect	0.819	0.781	0.83	0.44
YOLOv8n	Healthy	1	0.999	0.995	0.896
	Polluted	0.996	0.997	0.992	0.878
	Broken	0.996	1	0.992	0.844
	Surface Defect	0.995	0.998	0.995	0.828

TABLE VI  
PERFORMANCE COMPARISON OF YOLO MODELS

Parameters	Model Name				
	YOLOv3	YOLOv5	YOLOv6	YOLOv7	YOLOv8n
Precision	0.993	0.979	0.984	0.942	0.997
Recall	0.974	0.979	0.982	0.935	0.999
mAP@50	0.975	0.987	0.985	0.948	0.994
mAP@50-95	0.741	0.721	0.811	0.64	0.862
Layers	190	267	142	208	168
Param (M)	61.51	46.12	16.29	6.0	3.0
Flops (G)	154.6	107.7	44	13	8.1
Inference Time (sec)	9.6	3.5	3.4	3.7	2.08

TABLE VII  
CLASSIFICATION INDICES OF THE YOLOv8N MODEL

Performance Indices (%)	Individual Classes				YOLOv8n
	Healthy	Polluted	Broken	Surface Defect	Overall
Accuracy	0.9996	0.9983	0.9996	0.9990	0.9991
Error	0.0004	0.0017	0.0004	0.0010	0.0009
Recall	0.9993	0.9872	1	1	0.9965
Specificity	1	0.9996	0.9996	0.9986	0.9994
Precision	1	0.9967	0.9967	0.9965	0.9974
F1-Score	0.9996	0.9919	0.9983	0.9982	0.997
FM	0.9996	0.9919	0.9983	0.9982	0.997
MCC	0.9993	0.9910	0.9981	0.9975	0.9964
k	0.9993	0.9910	0.9981	0.9975	0.9964

### C. Comparative Analysis With SOTA Models

To assess the effectiveness of the approach, a comparative analysis was conducted on state-of-the-art (SOTA) models, including Faster R-CNN and SSD. The results of this analysis are presented in Table VIII. Furthermore, the proposed model demonstrates superior performance compared with ML, pretrained CNN, and hybrid models, as evidenced in Table IX.

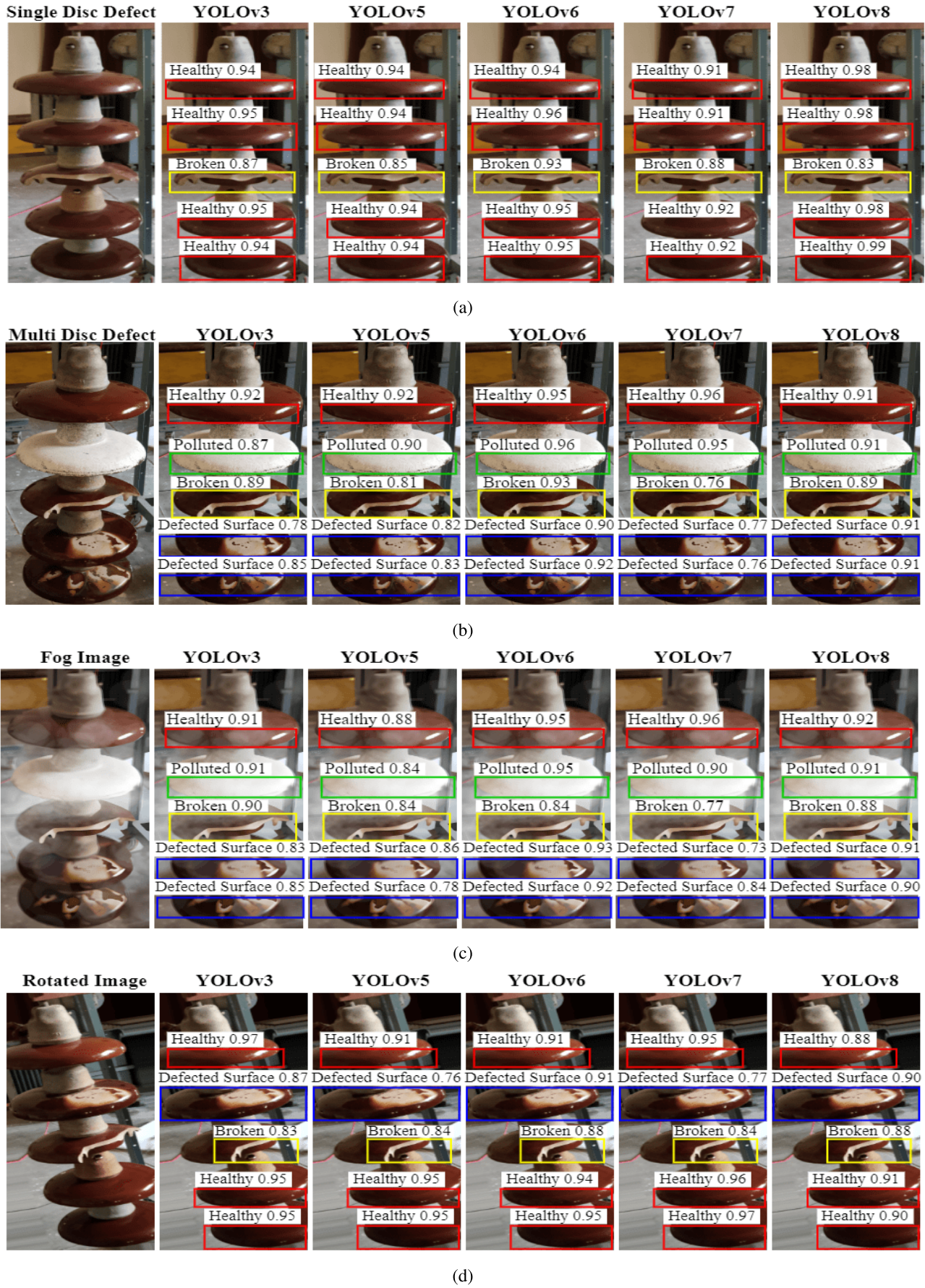


Fig. 8. Detection results on the test set using different YOLO models. (a) Single-disk defect. (b) Multidisk defect. (c) Fog image. (d) Rotated image.

		True Class			
		Healthy	Polluted	Broken	Surface Defect
Predicted Class	Healthy	3057	0	0	0
	Polluted	2	618	0	0
Broken	0	2	613	0	0
Surface Defect	0	6	0	1722	

Fig. 9. Confusion matrix of the YOLOv8n model.

TABLE VIII  
PERFORMANCE COMPARISON WITH DIFFERENT  
OBJECT DETECTION METHODS

Object Detector Type	Model Name	mAP@50	mAP@50-95
Two-stage	Faster R-CNN	0.9720	0.815
Single-stage	SSD	0.9810	0.8260
Proposed	YOLOv8n	0.994	0.862

TABLE IX  
PERFORMANCE COMPARISON WITH THE EXISTING METHODS

Ref.	Method	Dataset	Insulator Type	Defects	mAP (%)
[4]	ML (RF)	Private	Glass	Multi Class	80
[6]	Pre-trained CNN (ResNet 18)	Private	Glass	Single Class	95.1
[16]	YOLOv3	Public (CPLID)	Porcelain	Two Class	82.61
[13]	Hybrid-YOLO	Public (IDID)	Porcelain	Three Class	95.74
Proposed	YOLOv8n	Private	Porcelain	Multi Class	99.4



Fig. 10. YOLOv8n prediction for IDID image set [20]. (a) Broken. (b) Defected surface.

#### D. Results on Public Dataset

The proposed model was evaluated on the IDID dataset [20], achieving the mAPs of 84.5%, 84.9%, and 89% for defected surface, broken, and healthy insulators, respectively. In addition, on the CPLID image set [21], it achieved the mAPs of 98.2% for healthy insulators and 99.5% for defective insulators. Figs. 10 and 11 show the insulator defect classes with the confidence scores. These results proved the model's ability for untrained and unseen images.

#### E. Real-Time Monitoring With Hexacopter

Fig. 12 illustrates the ground control station (GCS) connected to the hexacopter via the telemetry module, with an added dongle arrangement establishing a remote connection

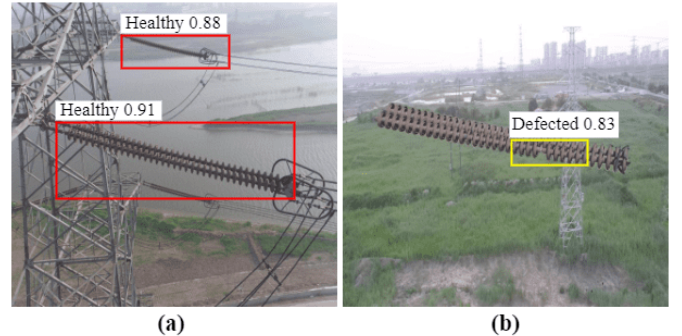


Fig. 11. YOLOv8n prediction for CPLID image set [21]. (a) Healthy insulator. (b) Defected insulator.

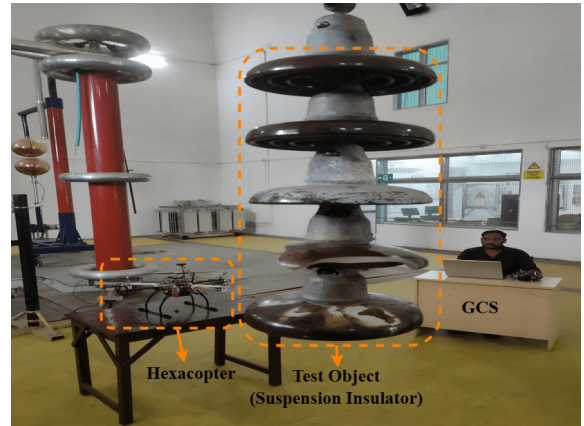


Fig. 12. Overall experiment setup.

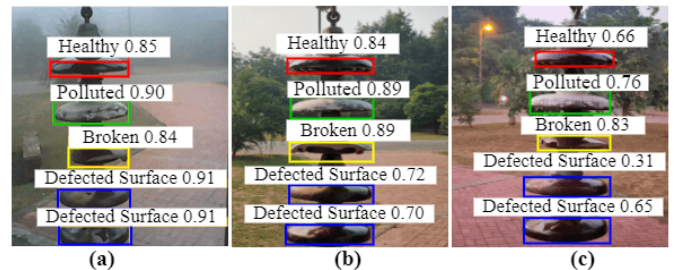


Fig. 13. Hexacopter's prediction for different times of the day. (a) Morning. (b) Afternoon. (c) Evening.

between the Raspberry Pi 4 and GCS. In Fig. 13, real-time detection of insulator defects using the hexacopter shows success in detecting defects with high precision in various environmental conditions: morning, afternoon, and evening replicating real-world scenarios of fog, sunlight, and low light.

#### V. CONCLUSION

This study presented a real-time condition monitoring system for transmission line insulators, which utilized the single-stage YOLO object detection model in conjunction with a hexacopter. The following conclusion were drawn from the study.

- 1) An insulator dataset consisting of 6020 images with various conditions, including clean, polluted, broken, and surface defects, was created to train the detector model.

- 2) This study employed augmentation methods as image preprocessing to mitigate the problem of overfitting.
- 3) Experimental results prove that the YOLOv8n model outperforms other single-stage object detectors with 99.4% of mAP@50 because of its transformer-based architecture design.
- 4) Finally, the suggested model was loaded into the Raspberry Pi 4 mounted on the hexacopter to inspect the outside insulator in real time.
- 5) The public dataset, such as IDID and CPLID, was used to test the detector model's robustness, and the results revealed an overall mAP of 86.13% and 98.85%, respectively.

In future research, the study aims to broaden its scope by integrating advanced deep neural models, such as hybrid models, GANs, and DETR, to address challenges related to identifying multiple defects on the same disk and detecting small defects with occlusion in the background.

## REFERENCES

- [1] J. Liu, M. Hu, J. Dong, and X. Lu, "Summary of insulator defect detection based on deep learning," *Electric Power Syst. Res.*, vol. 224, Nov. 2023, Art. no. 109688.
- [2] L. Yang, J. Fan, Y. Liu, E. Li, J. Peng, and Z. Liang, "A review on state-of-the-art power line inspection techniques," *IEEE Trans. Instrum. Meas.*, vol. 69, no. 12, pp. 9350–9365, Dec. 2020.
- [3] A. B. Alhassan, X. Zhang, H. Shen, and H. Xu, "Power transmission line inspection robots: A review, trends and challenges for future research," *Int. J. Electr. Power Energy Syst.*, vol. 118, Jun. 2020, Art. no. 105862.
- [4] D. Pernebayeva, A. Irmanova, D. Sadykova, M. Bagheri, and A. James, "High voltage outdoor insulator surface condition evaluation using aerial insulator images," *High Voltage*, vol. 4, no. 3, pp. 178–185, Sep. 2019.
- [5] X. Tao, D. Zhang, Z. Wang, X. Liu, H. Zhang, and D. Xu, "Detection of power line insulator defects using aerial images analyzed with convolutional neural networks," *IEEE Trans. Syst., Man, Cybern., Syst.*, vol. 50, no. 4, pp. 1486–1498, Apr. 2020.
- [6] Y. Cao, H. Xu, C. Su, and Q. Yang, "Accurate glass insulators defect detection in power transmission grids using aerial image augmentation," *IEEE Trans. Power Del.*, vol. 38, no. 2, pp. 956–965, Apr. 2023.
- [7] Z. Yuan et al., "CLAHE-based low-light image enhancement for robust object detection in overhead power transmission system," *IEEE Trans. Power Del.*, vol. 38, no. 3, pp. 2240–2243, Jul. 2023.
- [8] W. Zhao, M. Xu, X. Cheng, and Z. Zhao, "An insulator in transmission lines recognition and fault detection model based on improved faster RCNN," *IEEE Trans. Instrum. Meas.*, vol. 70, pp. 1–8, 2021.
- [9] X. Miao, X. Liu, J. Chen, S. Zhuang, J. Fan, and H. Jiang, "Insulator detection in aerial images for transmission line inspection using single shot multibox detector," *IEEE Access*, vol. 7, pp. 9945–9956, 2019.
- [10] D. Sadykova, D. Pernebayeva, M. Bagheri, and A. James, "IN-YOLO: Real-time detection of outdoor high voltage insulators using UAV imaging," *IEEE Trans. Power Del.*, vol. 35, no. 3, pp. 1599–1601, Jun. 2020.
- [11] X. Zhang et al., "InsuDet: A fault detection method for insulators of overhead transmission lines using convolutional neural networks," *IEEE Trans. Instrum. Meas.*, vol. 70, pp. 1–12, 2021.
- [12] J. Li, Y. Xu, K. Nie, B. Cao, S. Zuo, and J. Zhu, "PEDNet: A lightweight detection network of power equipment in infrared image based on YOLOv4-tiny," *IEEE Trans. Instrum. Meas.*, vol. 72, pp. 1–12, 2023.
- [13] B. J. Souza, S. F. Stefenon, G. Singh, and R. Z. Freire, "Hybrid-YOLO for classification of insulators defects in transmission lines based on UAV," *Int. J. Electr. Power Energy Syst.*, vol. 148, Jun. 2023, Art. no. 108982.
- [14] J. Zheng, H. Wu, H. Zhang, Z. Wang, and W. Xu, "Insulator-defect detection algorithm based on improved YOLOv7," *Sensors*, vol. 22, no. 22, p. 8801, Nov. 2022.
- [15] D. Waleed, S. Mukhopadhyay, U. Tariq, and A. H. El-Hag, "Drone-based ceramic insulators condition monitoring," *IEEE Trans. Instrum. Meas.*, vol. 70, pp. 1–12, 2021.
- [16] E. U. Rahman, Y. Zhang, S. Ahmad, H. I. Ahmad, and S. Jobaer, "Autonomous vision-based primary distribution systems porcelain insulators inspection using UAVs," *Sensors*, vol. 21, no. 3, p. 974, Feb. 2021.
- [17] C. Song, W. Xu, G. Han, P. Zeng, Z. Wang, and S. Yu, "A cloud edge collaborative intelligence method of insulator string defect detection for power IIoT," *IEEE Internet Things J.*, vol. 8, no. 9, pp. 7510–7520, May 2021.
- [18] J. Terven and D. Cordova-Esparza, "A comprehensive review of YOLO architectures in computer vision: From YOLOv1 to YOLOv8 and YOLO-NAS," 2023, *arXiv:2304.00501*.
- [19] A. B. Jung et al., "ImgAug," 2020. Accessed: Feb. 1, 2020. [Online]. Available: <https://github.com/aleju/imgaug>
- [20] D. Lewis and P. Kulkarni, "Insulator defect detection," *IEEE Dataport*, Aug. 2021, doi: [10.21227/vkdw-x769.s](https://doi.org/10.21227/vkdw-x769.s).
- [21] A. Raimundo, "Insulator data set—Chinese power line insulator dataset (CPLID)," *IEEE Dataport*, Feb. 2020, doi: [10.21227/qtxb-2s61](https://doi.org/10.21227/qtxb-2s61).



**Satyajit Panigrahy** (Graduate Student Member, IEEE) received the M.Tech. degree in power system engineering from the National Institute of Technology Hamirpur, Hamirpur, Himachal Pradesh, India, in 2019. He is currently pursuing the Ph.D. degree in electrical engineering with the National Institute of Technology Rourkela, Rourkela, India.

His research interests include pattern recognition, electrical and physicochemical characteristics analysis, and condition monitoring of high-voltage insulators using machine learning and deep learning methods.



**Subrata Karmakar** (Senior Member, IEEE) was born in 1981. He received the bachelor's degree (Hons.) in electrical engineering from Burdwan University, Bardhaman, India, in 2004, and the M.Tech. and Ph.D. degrees from the National Institute of Technology, Durgapur, India, in 2006 and 2011, respectively.

He is an Associate Professor with the Department of Electrical Engineering, National Institute of Technology Rourkela (NIT) Rourkela, Rourkela, India. His research interests include condition monitoring of high-voltage equipment, dielectric fluids, detection and localization of faults using signal processing, machine learning, and deep learning techniques in high-voltage power equipment.

Dr. Karmakar is currently a member of the IEEE Dielectric and Electrical Insulation Society (DEIS).